ELSEVIER

Solid State Ionics 149 (2002) 309–318

SOLID STATE IONICS

www.elsevier.com/locate/ssi

Analysis of the formation of ZrO_2:Y_2O_3 solid solution by the electrochemical impedance spectroscopy technique

F.C. Fonseca, E.N.S. Muccillo, R. Muccillo*

Multidisciplinary Center for the Development of Ceramic Materials, Energy and Nuclear Research Institute, CP 11049, Pinheiros, São Paulo 05422-970, SP, Brazil

Received 5 November 2001; received in revised form 18 March 2002; accepted 15 April 2002

Abstract

The formation of ZrO_2:8 mol% Y_2O_3 solid solution was studied by electrochemical impedance spectroscopy and X-ray diffraction analysis. The basic idea, starting from monoclinic zirconia and cubic yttria, was to follow the high-temperature substitution of Y^{3+} ions for Zr^{4+} ions in the zirconia matrix by determining the zirconia cubic phase content owing to X-ray diffraction and also the intragranular (bulk) electrical resistivity due to the increase of the concentration of oxygen ion vacancies. The cubic phase volume fraction and the bulk resistivity of the ZrO_2+Y_2O_3 polycrystalline specimens were found to depend on the square root of the time the specimen is kept at temperatures in the studied range: 1350–1450 °C. These results suggest a diffusion-controlled process during solid solution formation, allowing for the evaluation, by the impedance spectroscopy technique, of the thermal activation energy for diffusion of the slowest species (Zr^{4+}), in good agreement with the determination by other techniques.

PACS: 84.37; 66.30.N
Keywords: Impedance spectroscopy; Diffusion; Zirconia–yttria

1. Introduction

Zirconia-based solid electrolytes are used as electrochemical transducers in a series of devices like oxygen sensors, oxygen pumps and fuel cells [1]. Oxygen sensors find major applications in the steel making process (for the evaluation of the oxygen content in steel at high temperatures, ~1600 °C) and in the automotive industry (for the detection of by-products of the combustion process in car engines and for providing a feedback signal to the fuel injection system for fuel economy and decrease of environmental pollution) [2]. Oxygen pumps are used to provide known amounts of oxygen in closed systems and may be used for measuring the dependence of the electrical conductivity on the partial pressure of oxygen, and for thermogravimetric and X-ray analyses under controlled oxygen atmospheres [3,4]. Fuel cells can produce environmental clean electrical energy during conversion of oxygen and hydrogen to water [5]. All these applications rely on the fact that

* Corresponding author. Tel.: +55-11-3816-9343; fax: +55-11-3816-9343.
E-mail address: muccillo@usp.br (R. Muccillo).

0167-2738/02/$ - see front matter
PII: S0167-2738(02)00184-4

zirconia-based solid electrolytes are oxide ion conducting materials in a wide range of temperature and oxygen partial pressure. The defects responsible for the ionic conduction are oxygen-ion vacancies produced in zirconia by partial substitution of aliovalent (2+ or 3+) ions for zirconium ions. In particular, the 8 mol% Y_2O_3 substitution for ZrO_2, leads to a composition close to the lower limit for the stabilization of the zirconium oxide in the cubic structural phase with the highest value of electrical conductivity [6] in comparison to that of the tetragonal and monoclinic polymorphs of zirconia. This reaction can be described according to the Kroger–Vink notation [7]:

$$2Zr_{Zr}^{x} + O_{O}^{x} + Y_2O_3 \rightarrow 2Y_{Zr}' + V_{O}^{\cdot\cdot} + 2ZrO_2$$

Two things might be considered here. First, ZrO_2:8 mol% Y_2O_3 is the most important zirconia-based solid electrolyte for its electrical performance. Second, the stabilization of zirconia is the main phenomenon behind its electrical properties.

Mass transport in ceramics is important for their fabrication, functional properties and long term stability. Mass transport controls sintering rates, solid state reactions and grain growth [8]. Mass transport occurs via diffusion of chemical species. It is a fundamental process occurring in solid materials during processing—when atoms or ions exchange atomic sites—as well as in several applications of functional electrical ceramics when charge transfer across the solid occurs by ion migration. Diffusion is known to control mass transport mechanisms during sintering, grain growth, phase transitions and electrical conduction. The main experimental techniques for studying the diffusion of atomic species in solids are the radioactive tracer technique, electron microprobe analysis, imaging SIMS and autoradiography [8]. These techniques require depth profile measurements. In stabilized zirconium oxides, the oxygen ion has the highest mobility and its diffusion coefficient at 1000 °C is about six orders of magnitude higher than the diffusion coefficient of the cationic species [9]. The diffusion of the slower cations is the rate controlling step during important processes like rearrangement of atoms and structural homogenization, sintering kinetics, grain growth and phase stabilization [10,11]. Even though yttria-stabilized cubic zirconia (YSZ) is one of the most studied solid electrolytes due to the diversity of actual applications in industrial devices, there is not much available data on diffusion parameters [12].

The diffusion process as a function of temperature and time is quantitatively studied using Fick's second law

$$\frac{\partial C}{\partial t} = D\nabla^2 C$$

where $C \equiv C(r, t)$ is the concentration of the diffusing species at a diffusing depth r at time t and D is the chemical diffusion coefficient. That equation may be solved using suitable initial and boundary conditions depending on the particular system under study. The solutions of that equation indicate a dependence of the concentration of diffusing species on the square root of time [13,14]. The diffusion coefficient may be evaluated by determining the slope of the straight line that correlates the logarithm of concentration and $r/t^{1/2}$ [14].

A sintered polycrystalline solid electrolyte is composed basically of grains and internal surfaces like grain boundaries and pores. Impedance spectroscopy is a technique that allows for the determination of the individual contributions from grains (intragranular) and internal surfaces (intergranular) to the conductivity of a solid electrolyte [15–17].

There are many phenomena depending on mass transport that could be monitored to obtain a diffusion coefficient. Impedance spectroscopy has already been used to determine diffusion coefficients in a variety of electrochemical systems, including membranes, thin oxide films and alloys [17].

The main purpose of this paper is to study through impedance spectroscopy measurements the thermally assisted solid solution of zirconia+yttria polycrystalline specimens.

2. Experimental

Zirconium oxide (Fluka 99%) and yttrium oxide (99.9%) were used. These starting powders were dried at 100 °C for 1 h and stored in a dessicator. After weighing (Mettler AB 204) 50 g in the ZrO_2:8 mol% Y_2O_3 molar proportion, the mixed powders were attrition milled (Szegvasi attritor system) inside a

zirconia container with zirconia balls as milling medium. The milling conditions for a dispersion of 40 vol.% of mixed oxides in isopropyl alcohol were 400 rpm during 3 h. The milled suspension was dried at 90 °C in a roto-evaporator at 100 rpm. The resulting powder was deagglomerated in an agate mortar for 5 min. Green pellets of approximately 600 mg were prepared by uniaxial pressing in a stainless steel die at 100 MPa. Each ZrO_2+8 mol% Y_2O_3 pellet was placed inside an alumina boat with a zirconium oxide powder bed and covered with the same zirconium oxide powder for homogeneous distribution of heat. Each boat was inserted in an alumina tube placed inside a resistive tubular furnace (Lindberg model 54433) for heat treatments at 1350, 1400 and 1450 °C for several times. The heating rate was 5 °C/min and the cooling rate was that of the furnace switched off.

Structural phase characterization was performed at room temperature by X-ray diffraction measurements with a Bruker-AXS D8 Advance diffractometer. The flat surfaces of the pellets were positioned in a sample holder for a Bragg–Brentano θ–2θ configuration. The measurement conditions were: Cuk_α radiation at 40 kV–40 mA, 18–86° 2θ range, 0.05° 2θ step and 10 s of counting time per step.

Impedance spectroscopy measurements were carried out with a Hewlett Packard 4192A Impedance Analyzer connected to a series 900 model 362 HP controller. A special software was used to collect, store and analyze the (Z'', Z) data [18]. The analysis of a (Z'', Z') diagram consists in the deconvolution, in the frequency domain, of the impedance responses due to the intergranular and intragranular contributions, which are usually composed of overlapping semicircles. Pellets for impedance spectroscopy measurements had their parallel surfaces polished with sandpaper and ultrasonically cleaned with isopropyl alcohol. Silver electrodes were prepared by painting with colloidal silver and curing at 400 °C for 15 min for removal of the organic binder. The specimens (three at a time) were spring-loaded inside a sample chamber made of inconel 600 alloy and sintered high-alumina pieces. The sample chamber, with platinum (discs and wire) electrodes was inserted in a vertical tubular furnace for measurements in the 300–600 °C temperature range. Using a proportional–integral–differential control, the temperature control was better than 0.5 °C. The temperature of the specimens inside the sample chamber was monitored with a NBS calibrated chromel–alumel thermocouple with its sensing tip located at the closest equal distance from the three specimens. Another chromel–alumel with its sensing tip inserted in a dewar flask with liquid nitrogen provided a stable reference temperature. As no diffusional processes are expected to occur at temperatures chosen for impedance spectroscopy measurements, these measurements were performed after 30 min at each temperature. A further experimental precaution on the determination of the temperature of the specimens inside the sample chamber was taken by always placing in the sample chamber a sintered ZrO_2+8 mol% Y_2O_3 specimen with known (previously measured) impedance versus temperature profile. This procedure was found to give better temperature determination than simply by determining the electromotive force of the chromel–alumel thermocouple. The impedance spectroscopy diagrams were collected in the 5 Hz–13 MHz frequency range with input voltages in the 0.1–0.5 V range. The (Z'', Z') data consisted of 16 values per frequency decade and 5 s of time delay per collected frequency data.

3. Results and discussion

Fig. 1 shows the distribution of particle sizes of the zirconium oxide and yttrium oxide powders used in this work. In the same figure, the distribution of

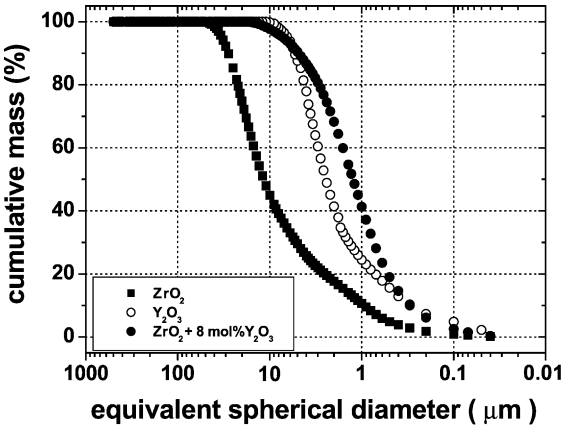

Fig. 1. Cumulative distribution of particle size of ZrO_2, Y_2O_3 and ZrO_2+8 mol% Y_2O_3 mixture after attrition milling.

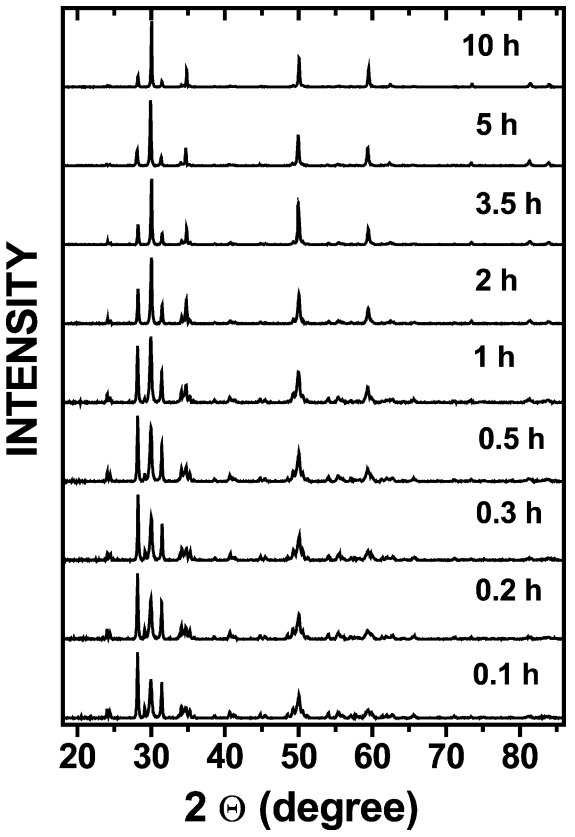

Fig. 2. X-ray diffraction patterns of ZrO_2+8 mol% Y_2O_3 pressed (attrition milled) ceramic pellets heat treated at 1350 °C for different times (0.1–10.0 h, bottom to top).

particle sizes of the ZrO_2+8 mol% Y_2O_3 mixture after attrition milling is also shown. The average particle sizes of ZrO_2, Y_2O_3 and the milled mixture were determined as 11.6, 2.4 and 1.2 μm, respectively. A reduction of the average particle size was achieved by attrition milling enabling better packing of the mixture for a better particle–particle interaction for the interdiffusion of the yttrium and zirconium ions. Green density of specimens was ~3.3 g/cm^3, which corresponds to ~55% of the theoretical density for ZrO_2+8 mol% Y_2O_3.

Fig. 2 shows X-ray diffraction patterns of pressed ZrO_2+8 mol% Y_2O_3 (attrition milled powders) pellets after heat treatments at 1350 °C for times from 6 min up to 10 h. For heating times up to 2 h, three structural phases are detected: monoclinic zirconia, cubic zirconia and cubic yttria. For increased heating times, the zirconia cubic phase content increases while the zirconia monoclinic phase and the yttria cubic phase contents decrease, as expected. This means that as the stabilization process of zirconia proceeds, yttrium ions are supplied to the zirconia matrix for solid solution formation, i.e., for the partial stabilization of zirconia in the cubic phase. Fig. 3 shows, in the 27.5–32 2θ range, details of some of the X-ray diffraction patterns depicted in Fig. 2. Even though the main diffraction lines due to yttrium oxide are not detected after heating times longer than 2 h, we consider that the yttria is still present as a second phase in the mixture. This assertion is based on the continuous increase of the main cubic zirconia diffraction lines for heating times longer than 2 h.

The determination of the relative cubic phase content (v_c) and monoclinic phase content (v_m=1−v_c) was done according to the following equation [19]:

$$v_m = 1.306X_m/(1 + 0.306X_m)$$

where

$$X_m = A/[A + I_c(111)]$$

and

$$A = I_m(-111) + I_m(111)$$

$I_{m,c}(hkl)$ stands for the X-ray diffraction intensity of the corresponding (hkl) plane.

In Fig. 4, the cubic phase content v_c is plotted as a function of the time the specimen is heated at 1350 °C

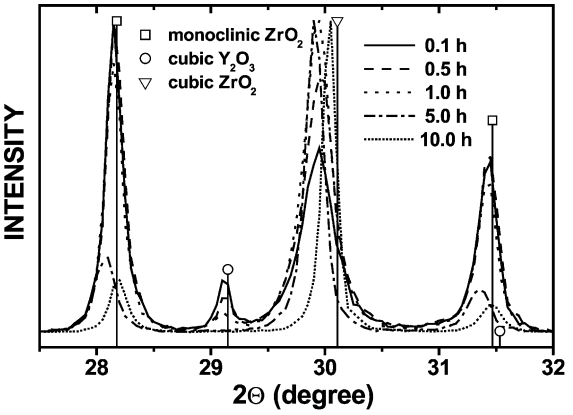

Fig. 3. X-ray diffraction patterns (2θ range: 27.5–32°) of ZrO_2+8 mol% Y_2O_3 pressed ceramic pellets heat treated at 1350 °C for 0.1, 0.5, 1.0, 5.0 and 10.0 h.

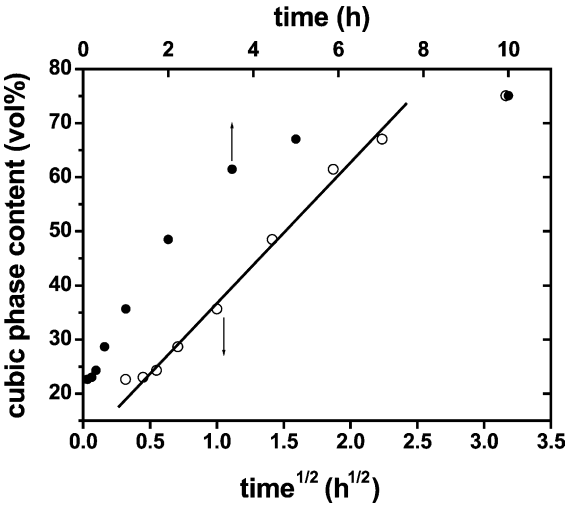

Fig. 4. Dependence of the cubic phase content on the time of heat treatment at 1350 °C of ZrO_2+8 mol% Y_2O_3 pressed ceramic pellets. The linear dependence is on the square root of time.

(top *x*-axis). The remarkable feature of this result is found when v_c is plotted as a function of the square root of the heating time (bottom *x*-axis). From 0.2 to 5 h, a linear dependence is found, an evidence that a diffusion process is responsible for the cubic phase formation at the expenses of the zirconia monoclinic and cubic yttria phases. The deviation in the linear dependence for times shorter than 0.2 h, i.e., a cubic phase content higher than expected, is probably due to the extra cubic phase formation by simply heating up the specimen to 1350 °C. The deviation found for times longer than 5 h at 1350 °C might be due to particle size effects: an external shell of the zirconia particles reaching the saturation solid solution (cubic phase) formation at that temperature would inhibit the yttrium ions to further diffuse into the core of the particles and, consequently, inhibit the cubic phase formation. Further experimental work is necessary to check this assumption. It should be noticed that diffusion processes based on the $t^{1/2}$ dependence of concentration of moving species in solids have already been reported on a series of compounds [20,21].

Unless otherwise reported, all impedance measurements of the specimens heated at 1350, 1400 and 1450 °C described in this paper were measured at 470 °C. That temperature is high enough for detecting both intergranular and intragranular contributions to the conductivity due to O^{2-} ion migration—that is, the specimen is in the electrolytic region—and low enough to keep constant the phase content achieved at the heating temperature ($T \geq 1350$ °C).

Fig. 5a, b and c shows impedance diagrams (the imaginary part of the impedance as a function of the real part of the impedance), also called Nyquist plots, of ZrO_2+8 mol% Y_2O_3 pressed pellets after heating to 1350 °C (Fig. 5a), 1400 °C (Fig. 5b) and 1450 °C (Fig. 5c) for 0.2, 0.5, 1.0, 2.0 and 5.0 h. Specimens

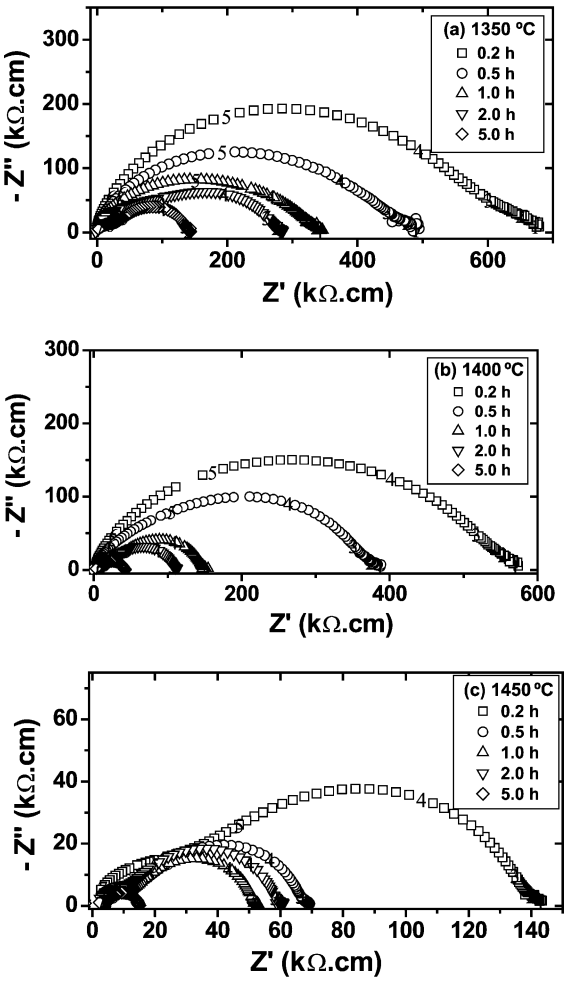

Fig. 5. Impedance diagrams of ZrO_2+8 mol% Y_2O_3 pressed pellets after heat treatments at (a) 1350, (b) 1400 and (c) 1450 °C for different times. Diagrams obtained at 470 °C. Numbers substituting symbols denote the logarithm of frequency.

prepared with heating times different than those shown in Fig. 5 had the impedance diagrams also measured and the data follow the same trend. These results are not shown in Fig. 5 for the sake of clarity. The impedance diagrams show that both imaginary and real components decrease with increasing the time at any of the investigated temperatures. The decrease of the real part of the impedance, which corresponds to a decrease of the electrical resistance of the specimens, is due to the stabilization of the cubic phase or to the increase of the volume fraction of the oxygen ion conducting (cubic) phase. The analysis of the diagrams were made considering a one semicircle model for samples heated at 1350 and 1400 °C for times $t<0.5$ h. For times longer than these, two semicircles were resolved. It is important to point out that the diagrams corresponding to samples heated at 1350 °C for $0.5 \leq t \leq 1$ h are not so evident to resolve. It is necessary at least a two components model to describe those diagrams, but a three components model, considering a semicircle due to monoclinic zirconia blocking of charge carriers at intermediate frequencies ($\sim 10^5$ Hz), could be considered. This three components model has already been reported [22] but, in the present study, both further investigation and more experimental data are necessary to assure this behavior and such an interpretation would be beyond the scope. Since the main conclusions in

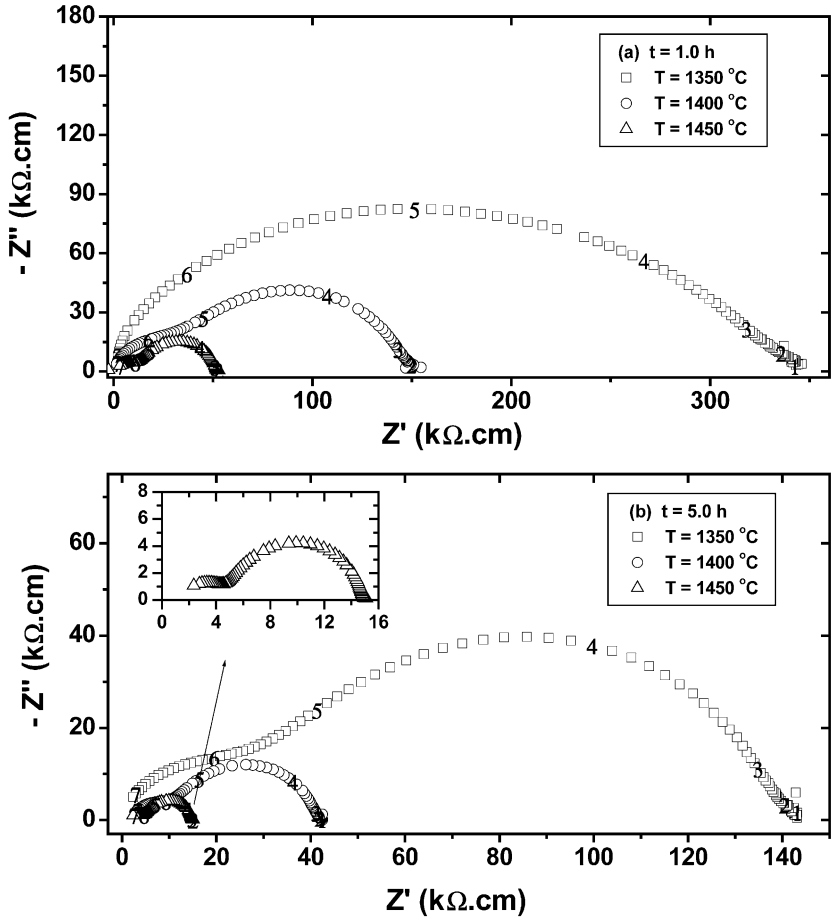

Fig. 6. Impedance diagrams of ZrO_2+8 mol% Y_2O_3 pressed pellets after heat treatments during (a) 1.0 and (b) 5.0 h at different temperatures. Diagrams obtained at 470 °C. Numbers substituting symbols denote the logarithm of frequency.

this work are based on a series of samples with various heating times and temperatures which resulted in well-resolved diagrams using a two components model, this model was adopted to fit all diagrams of specimens heated for times $t > 0.5$ h. The high-frequency semicircle is due to the intragranular ionic conduction in stabilized zirconia because this is the only conducting phase present in the specimen (cf. the X-ray diffraction results, Fig. 2). It could not be due to any contribution of the conductivity of the monoclinic phase because the conductivity of the monoclinic zirconia is known to be much lower than that of cubic zirconia [23]. The low frequency semicircle is clearly due to blocking of charge carriers at interfaces and second phases in the non-fully sintered ZrO_2+Y_2O_3 ceramic pellets. These interfaces are nonconducting regions like grain boundaries or pores; the second phases are the insulating yttria and the monoclinic zirconia. Several studies on the use of the impedance spectroscopy technique to the study of sintering of zirconia–yttria ceramics have been reported [24–33]. The isothermal sintering in the last stage of the sintering process leads to pore elimination as a consequence of the increase of the average grain size [28]. It has already been shown that for zirconia–yttria specimens the intragranular (bulk) resistivity does not change with sintering time in the last stage of sintering [33]. That means that the decrease in the intragranular resistivity (high-frequency region in Fig. 5) is a consequence of the stabilization of zirconia and not due to grain growth.

Fig. 6 shows the impedance diagrams measured after heat treating the specimens at three different temperatures for two fixed times: 1.0 h (Fig. 6a) and 5.0 h (Fig. 6b). Here, the temperature evolution of the total electrical resistance of the specimens can be seen, suggesting a strong temperature dependence of the resistivity, an Arrhenius type, for example, as described below.

The intragranular (HF) and the intergranular (LF) resistivity values were determined after deconvolution of the impedance diagrams measured at 470 °C in specimens heat treated at different temperatures and times.

Fig. 7 shows values of the intergranular and intragranular resistivities as a function of the square root of the time the ZrO_2+8 mol% Y_2O_3 specimens are heat treated at 1350 °C (Fig. 7a), 1400 °C (Fig. 7b) and

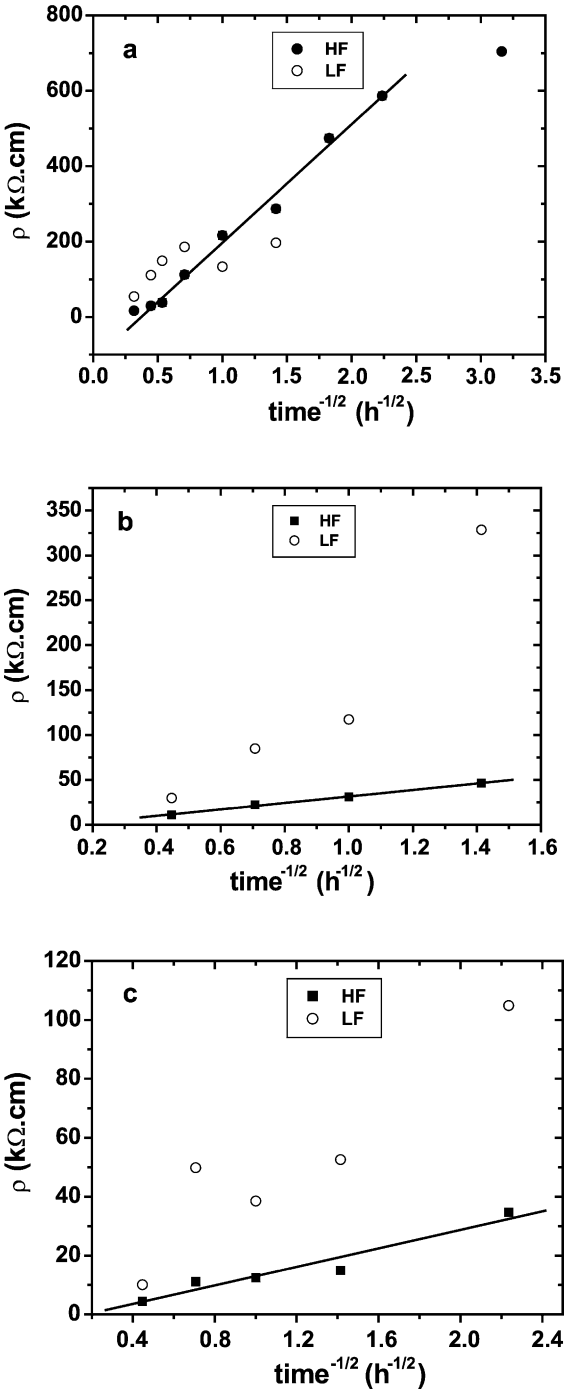

Fig. 7. Dependence of the intragranular (HF) and intergranular (LF) resistivity on the reciprocal of the square root of the time of heat treatment at (a) 1350, (b) 1400 and (c) 1450 °C of ZrO_2+8 mol% Y_2O_3 pressed pellets. Impedance spectroscopy data measured at 470 °C.

1450 °C (Fig. 7c). A linear dependence is found for data taken from the impedance diagrams measured at 470 °C (Fig. 7a) and at 560 °C (Fig. 7b). These results are similar to the ones shown in Fig. 4 for the cubic phase content. The first conclusion is that the increase of the conductivity depends directly on the increase of the cubic phase content. Moreover, it can be seen that the intragranular (HF) data and only these data show a linear dependence, suggesting a diffusion process takes place in the bulk of the specimens.

The blocking factor α_R and the frequency factor α_f were determined from the impedance diagrams. The blocking factor is defined as the ratio of the intergranular electrical resistance to the total electrical resistance and is proportional to the density of blocked charge carriers. The frequency factor is defined as the ratio of the relaxation frequency determined at the apex of the intergranular semicircle to that of the intergranular semicircle. It has already been shown that the blocking factor is proportional to the intergranular average blocking surface (i.e., to the intergranular surface). The frequency factor, on the other hand, has been shown to be proportional to the intergranular average distance [34,35]. Their product is then considered to be proportional to the intergranular volume [34]. These parameters are expressed as:

$$\alpha_R = \frac{R_{LF}}{R_{HF} + R_{LF}};\ \alpha_f = \frac{f_{0\ LF}}{f_{0\ HF}}.$$

The product $\alpha_R\alpha_f$ has already been used to describe pore elimination and grain growth processes in zirconia-based materials [25,33]. In the present study, only qualitative variations of the product $\alpha_R\alpha_f$ are taken into account.

Fig. 8 shows the $\alpha_R\alpha_f$ product as a function of the reciprocal of the square root of the time of heat treating ZrO_2+8 mol% Y_2O_3 pressed pellets at 1350, 1400 and 1450 °C. The value of the $\alpha_R\alpha_f$ product, i.e., the volume fraction of the blockers (pores and insulating phases) decreases for increasing times of heat treatments. A linear dependence is found for the reciprocal of the square root of time. This is an indication that the blocking parameters can also be used for following the solid solution formation in zirconia–yttria solid electrolytes. The advantage of using these parameters is that they do not depend on the geometrical factor of the specimens [36].

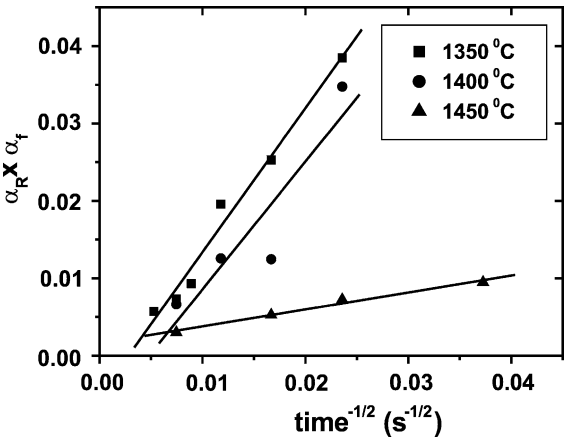

Fig. 8. Dependence of the $\alpha_R\alpha_f$ product (α_R is the blocking factor, α_f is the frequency factor) on the reciprocal of the square root of time of heat treatment of ZrO_2+8 mol% Y_2O_3 pressed pellets. Temperatures of heat treatment: 1350, 1400 and 1450 °C. See text for details.

The thermal activation energies were determined from Arrhenius plots of the intergranular and intragranular resistivities. The values are approximately 1 eV, a typical value for the activation energy of oxygen ions in zirconia solid electrolytes. The intergranular activation energy is 10% larger than the intragranular activation energy, as expected for zirconia [36].

Fig. 9 shows the intragranular electrical resistivity data of ZrO_2+8 mol% Y_2O_3 pressed pellets as a function of the reciprocal heat treatment temperature for three temperatures: 1350, 1400 and 1450 °C. Even though data were collected for isothermal treatments at these temperatures for several periods of time, the figure shows only data for 5-h treatments, for sake of clarity. Similar behavior was found for specimens heat treated at these temperatures for different periods of time.

The impedance spectroscopy measurements were performed at 370, 420, 470 and 515 °C. Even though the analysis takes into account only three temperatures, the intragranular resistivity shows a linear dependence with the reciprocal of the absolute temperature, a clear indication that an Arrhenius-type thermally activated process takes place during solid solution formation. The determination of the thermal activation energy was determined as 4.6±0.3 eV, in good agreement with the value recently reported for the zirconium ion diffusion in single crystalline [12]

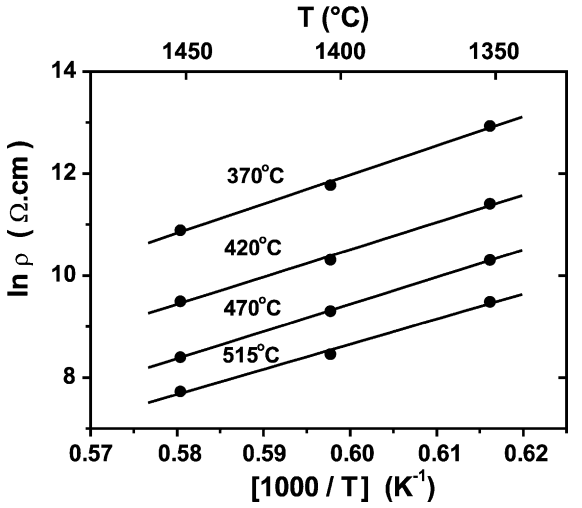

Fig. 9. Intragranular electrical resistivity of ZrO_2+8 mol% Y_2O_3 pressed pellets as a function of the reciprocal heat treatment temperature (1350 °C/5 h, 1400 °C/5 h and 1450 °C/5 h). Temperature of impedance spectroscopy measurement, from top to bottom: 370, 420, 470 and 515 °C. See text for details.

and polycrystalline [9] ZrO_2:8 mol% Y_2O_3 specimens: 4.5±0.2 and 4.8 eV, respectively. These two reported values were determined by the radioactive tracer technique. Values determined by other techniques are also in that range (Cf. Table 1 in Ref. [12]). It is known that the oxygen ion is the species with higher mobility in zirconia–yttria, controlling the electrolytic processes in this solid electrolyte material. For an effective mass transport required for densification and solid solution formation, all species must take part in the diffusion processes. This is the reason for the whole rates of sintering and solid solution processes are controlled by the diffusion of the slowest species, zirconium ions in the zirconia–yttria system [37]. The measurement of the intragranular resistivity by impedance spectroscopy in mixtures of zirconia and yttria powders isothermally treated at different temperatures and times is a way to determine the thermal activation energy for diffusion of the zirconium ion.

4. Conclusions

The formation of the solid solution of zirconium oxide and yttrium oxide was successfully evaluated by impedance spectroscopy measurements on pellets annealed at different temperatures and times. The results were analyzed using the amplitudes of the main diffraction lines of the fluorite structure of zirconia–yttria and the parameters evaluated from the impedance diagrams: intergranular and intragranular resistivities, blocking factor and frequency factor. A good correlation was found between the intragranular (bulk) resistivity and the square root of the time for interdiffusing Y^{3+} and Zr^{4+}, allowing for the determination of the thermal activation energy for diffusion of the slowest species (Zr^{4+} ions).

Depth profiling, consisting on the determination of the concentration of the diffusant species as a function of position following one-dimensional diffusion from a planar source, is known to give the most reliable data for the evaluation of diffusion coefficients. Experiments, using the sectioning technique followed by the indirect determination of the diffusant concentration by X-ray diffraction and impedance spectroscopy are under way.

Acknowledgements

We give thanks to CNEN, FAPESP (97/00727-3, 98/14324-0 and 99/10798-0), CNPq (306496/88-7 and 300934/94-7) and PRONEX for financial support and scholarships.

References

[1] A.H. Heuer, L.W. Hobbs (Eds.), Science and Technology of Zirconia I, Advances in Ceramics, vol. 3, The American Ceramic Society, Columbus, OH, USA, 1981, pp. 1–475.
[2] E.C. Subbarao (Eds.), Solid Electrolytes and their Applications, Plenum, New York, USA, 1980, pp. 1–298.
[3] J. Fouletier, H. Seinera, M. Kleitz, J. Appl. Electrochem. 5 (1975) 111.
[4] S.H. Chu, S.A. Seitz, J. Solid State Chem. 23 (1978) 297.
[5] S.C. Singhal, in: S.C. Singhal, M. Dokiya (Eds.), Proc. Sixth Int. Symp. Solid Oxide Fuel Cells (SOFC VI), The Electrochemical Society, New Jersey, 1999, p. 39.
[6] E.C. Subbarao, in: A.H. Heuer, L.W. Hobbs (Eds.), Science and Technology of Zirconia I, Advances in Ceramics, vol. 3, The American Ceramic Society, Columbus, OH, USA, 1981, p. 1.
[7] F.A. Kroger, H.J. Vink, in: F. Seitz, D. Turnbull (Eds.), Solid State Physics, vol. 3, Academic Press, New York, USA, 1956, p. 307.

[8] A. Atkinson, in: R.W. Cahn, P. Haasen, E.J. Kramer (Eds.), Materials Science and Technology, A Comprehensive Treatment, Structure and Properties of Ceramics, vol. 11, VCH Verlagsgesellschaft, Weinheim, Germany, 1994, p. 295, M.V. Swain (Vol. Ed.).
[9] A. Lakki, R. Herzog, M. Weller, H. Schubert, C. Reetz, O. Görke, M. Kilo, G. Borchardt, J. Eur. Ceram. Soc. 20 (2000) 285.
[10] S.J. Rothman, in: G.E. Murch, A.S. Nowick (Eds.), Diffusion in Crystalline Solids, Academic Press, Orlando, FL, USA, 1984, pp. 1–61.
[11] Hj. Matzke, in: O.T. Sorensen (Eds.), Nonstoichiometric Oxides, Academic Press, New York, USA, 1981, pp. 155–231.
[12] M. Kilo, G. Borchardt, B. Lesage, O. Kaïtasov, S. Weber, S. Scherrer, J. Eur. Ceram. Soc. 20 (2000) 2069.
[13] Y. Adda, J. Philibert, La Diffusion Dans Les Solides, Presses Universitaires de France, Paris, France, 1966.
[14] S.J. Rothman, in: G.E. Murch, A.S. Nowick (Eds.), Diffusion in Crystalline Solids, Academic Press, Orlando, FL, USA, 1984, p. 5.
[15] J.E. Bauerle, J. Phys. Chem. Sol. 30 (1969) 2657.
[16] M. Kleitz, H. Bernard, E. Fernandez, E. Schouler, in: A.H. Hobbs, L.W. Hobbs (Eds.), Science and Technology of Zirconia I, Advances in Ceramics, vol. 3, The American Ceramic Society, Columbus, OH, USA, 1981, p. 310.
[17] I.D. Raistrick, in: J.R. Macdonald (Eds.), Impedance Spectroscopy—Emphasizing Solid Materials and Systems, Wiley Interscience, New York, USA, 1987, p. 29.
[18] M. Kleitz, J.H. Kennedy, in: P. Vashishta, J.N. Mundy, G.K. Shenoy (Eds.), Fast Ion Transport in Solids, Elsevier, North Holland, The Netherlands, 1979, p. 185.
[19] R.C. Garvie, P.S. Nicholson, J. Am. Ceram. Soc. 55 (1972) 303.
[20] A.D. Smigelskas, E.O. Kirkendall, Trans. Am. Inst. Min. Metall. Eng. 171 (1947) 130.
[21] J.A.M. van Roosmalen, E.H.P. Cordfunke, Solid State Ionics 52 (1992) 303.
[22] E.N.S. Muccillo, M. Kleitz, J. Eur. Ceram. Soc. 16 (1996) 453.
[23] F.K. Moghadam, T. Yamashita, D.A. Stevenson, in: A.H. Heuer, L.W. Hobbs (Eds.), Science and Technology of Zirconia I, Advances in Ceramics, vol. 3, The American Ceramic Society, Columbus, OH, USA, 1981, p. 364.
[24] S.P.S. Badwal, Solid State Ionics 76 (1995) 67.
[25] M.C. Steil, F. Thévenot, M. Kleitz, J. Electrochem. Soc. 144 (1997) 390.
[26] A.I. Ioffe, M.V. Inozemtzev, A.S. Lipilin, M.V. Perfilev, S.V. Karpachov, Phys. Status Solidi A 30 (1975) 87.
[27] M.J. Verkerk, B.J. Middelhuis, A.J. Burggraaf, Solid State Ionics 6 (1982) 159.
[28] M.J. Verkerk, A.J.A. Winnubst, A.J. Burggraaf, J. Mater. Sci. 17 (1982) 3113.
[29] E.J.L. Schouler, M. Mesbahi, G. Vitter, Solid State Ionics 9–10 (1983) 989.
[30] S.P.S. Badwal, J. Drennan, J. Mater. Sci. 22 (1987) 3231.
[31] M. Gödickemeier, B. Michel, A. Orliukas, P. Bohac, K. Sasaki, L. Gauckler, H. Heinrich, P. Sxhwander, G. Kortorz, H. Hofmann, O. Frei, J. Mater. Res. 9 (1994) 1228.
[32] M. Aoki, Y.-M. Chiang, I. Kosacki, L.J.-R. Lee, H. Tuller, Y. Lu, J. Am. Ceram. Soc. 79 (1996) 1169.
[33] D.Z. Florio, R. Muccillo, Solid State Ionics 123 (1–4) (1999) 301–305.
[34] M. Kleitz, L. Dessemond, M.C. Steil, Solid State Ionics 75 (1995) 107.
[35] M. Kleitz, M.C. Steil, J. Eur. Ceram. Soc. 17 (1997) 819.
[36] M. Kleitz, L. Dessemond, M.C. Steil, F. Thévenot, in: R.A. Gerhardt, S.R. Taylor, E.J. Garboczi (Eds.), Mater. Res. Symp. Proc. vol. 411, 1996, p. 269.
[37] F.R. Chien, A.H. Heuer, Philos. Mag. A 73 (1996) 681.